Measurement of the lattice parameter of a silicon crystal

2009 New J. Phys. 11 053013

(http://iopscience.iop.org/1367-2630/11/5/053013)

New Journal of Physics
The open-access journal for physics

Measurement of the lattice parameter of a silicon crystal

E Massa[1,4], G Mana[1], U Kuetgens[2] and L Ferroglio[1,3]

[1] INRIM—Istituto Nazionale di Ricerca Metrologica, Str. delle Cacce 91, 10135 Torino, Italy

[2] PTB—Physikalish-Technische Bundesanstalt, Bundesalle 100, 38116 Braunschweig, Germany

[3] Politecnico di Torino, c.so Duca degli Abruzzi 24, 10129 Torino, Italy

E-mail: e.massa@inrim.it

New Journal of Physics **11** (2009) 053013 (12pp)
Received 2 February 2009
Published 27 May 2009
Online at http://www.njp.org/
doi:10.1088/1367-2630/11/5/053013

Abstract. The silicon crystal WASO04 is a reference in the adjustment of fundamental physical constants, but its lattice parameter has never been measured in absolute terms. In the framework of an international project meant to base the kilogram definition on the molar volume and the lattice parameter of ^{28}Si, the WASO04 crystal has been used to manufacture an interferometer prototype for the performance testing and the fine-tuning of a new experimental apparatus for lattice parameter measurements by combined x-ray and optical interferometry. The present paper discusses the test results and gives an accurate lattice parameter determination. With respect to previous determinations, the value obtained, $d_{220}(\mathrm{WASO04}) = 192.015\,570\,2(10)$ pm, displays a four-fold improvement in accurracy.

[4] Author to whom any correspondence should be addressed.

Contents

1. Introduction

To determine the Avogadro constant, N_A, to an accuracy allowing the kilogram definition to be based on the atomic mass of the ^{28}Si atom [1, 2], several metrology institutes are participating in a research project (International Avogadro Coordination, IAC) for the determination of N_A with the use of a highly enriched ^{28}Si crystal [3]. In this framework, the relative uncertainty of the Si lattice parameter must be reduced to 3×10^{-9}. In addition, an accurate value of the Si lattice parameter is relevant for determining the relative atomic mass of the neutron and the fine-structure constant [4]. With this in view, the measurement capabilities of the Istituto Nazionale di Ricerca Metrologica (INRIM) were extended and an interferometer prototype with an unusually long analyzer crystal was manufactured from a high-purity natural Si crystal, named WASO04, which was purposely grown for N_A determination [5, 6].

INRIM measured the (220) lattice plane spacing of WASO04—d_{220}, which is related to the lattice parameter by the equation $a_0 = \sqrt{8}d_{220}$—in 2006; the result is given in [7]. However, owing to imperfect design of the x-ray interferometer, which required subsequent reshaping, the measured value was never completely relied upon and it was not included in the 2006 adjustment of the recommended values of the fundamental physical constants [4]. Consequently, the input lattice parameter value for the adjustment was based on extrapolation from the residual carbon and oxygen contamination and on lattice comparisons—carried out by the Physikalish-Technische Bundesanstalt (PTB) via x-ray double crystal diffractometry—against crystals the lattice parameters of which were measured in absolute terms [4, 5].

To operate a separate-crystal interferometer of such a size was a formidable task: the result is a system that accurately measures and controls changes in the position and alignment of the interferometer crystals at the sub-atomic level and over distances as large as 5 cm. Test measurements were performed to verify and demonstrate the apparatus performance and to assess the experiment limits. The results, as well as the first absolute determination of the WASO04 lattice parameter, are given in the present paper. They indicate that, notwithstanding the modification during measurement, our previous 2006 value was correct.

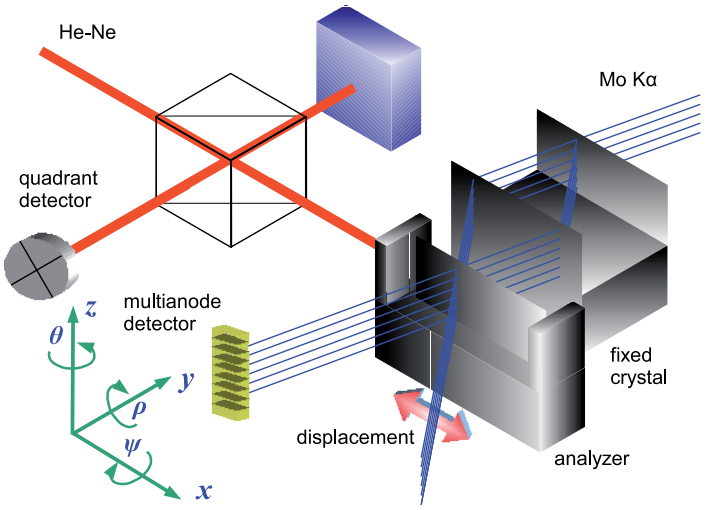

Figure 1. Combined x-ray and optical interferometer. The analyzer crystal moves along the line indicated by the arrow.

2. Experimental apparatus

2.1. Combined x-ray and optical interferometry

A combined x-ray and optical interferometer is shown in figure 1. It consists of three crystals cut so that the (220) planes are orthogonal to the crystal surfaces. X-rays from a 17 keV Mo Kα source having a (10×0.1) mm^2 line focus are split by the first crystal and then recombined, via two transmission crystals, by the third, called the analyzer. When the analyzer crystal is moved along a direction orthogonal to the (220) planes, a periodic variation in the transmitted and diffracted x-ray intensities is observed, the period being the diffracting-plane spacing. The analyzer embeds front and rear mirrors, so that its displacement is measured by optical interferometry; the necessary picometer resolution is achieved by polarization encoding and phase modulation. The laser source realizes the meter by definition; it operates in single-mode configuration and its frequency is stabilized against that of a recommended transition of the $^{127}I_2$ molecule. This ensures the calibration of the optical interferometer with a negligible uncertainty. To eliminate the adverse influence of the refractive index of air, the experiment is carried out in a vacuum.

According to the measurement equation

$$d_{220} = (m/n)\lambda/2, \tag{1}$$

the larger the crystal displacement, the higher the resolution. In equation (1), n is the number of x-ray fringes of the d_{220} period in a crystal displacement spanning m optical fringes of the $\lambda/2$ period. The interferometer operation was extended up to displacements of 5 cm. This magnification makes more numerous systematic effects visible and reproducible. In addition, it allows wider crystal parts to be surveyed, thus increasing confidence in the crystal perfection and in the mean value of the lattice parameter. This measurement capability is obtained by means of a guide where an L-shaped carriage slides on a quasi-optical rail. The successful operation of a separate-crystal interferometer is a challenge: the fixed and movable crystals must be so faced to allow the atoms to recover their exact position in the initial single crystal

Table 1. Crystal WASO04—relevant data.

Orientation	100
Type	*n*
Crystal length and diameter	170 cm, 10.3 cm
Growth rate	2.5 mm min^{-1}
Growth atmosphere	Ar, a few bars pressure
Resistivity	3.3(2) kΩ cm
Carbon	$2.8(4) \times 10^{15}$ cm^{-3}
Oxygen	$1.1(2) \times 10^{15}$ cm^{-3}
Nitrogen	$0.7(1) \times 10^{15}$ cm^{-3}
Boron	$< 1 \times 10^{12}$ cm^{-3}
Phosphorus	$< 3 \times 10^{12}$ cm^{-3}
Hydrogen	$< 3 \times 10^{12}$ cm^{-3}
Vacancies and self-interstitial	$< 1 \times 10^{14}$ cm^{-3}

and they must be kept aligned notwithstanding vibrations and displacements. Hence, an active tripod with three piezoelectric legs rests on the carriage. Each leg expands vertically and shears in the two transverse directions, thus allowing compensation for the sliding errors and electronic positioning of the x-ray interferometer over six degrees of freedom to atomic-scale accuracy. Crystal displacement, parasitic rotations and transverse motions are sensed via laser interferometry and by capacitive transducers. Feedback loops provide picometer positioning, nanoradian alignment and interferometer movement with nanometer straightness.

2.2. The WASO04 interferometer

The x-ray interferometer was manufactured by PTB from the high-purity WASO04 crystal, grown and purified by application of the float-zone technique by Wacker Siltronic in January 1995. The crystal was grown with nitrogen doping to prevent precipitation of vacancies and self-interstitials (swirl defects); some data are summarized in table 1 and figure 2. More detailed information about the crystal characterization can be found in [5]. The homogeneity of the lattice parameter was investigated by PTB and the National Institute of Standards and Technology (NIST) [8, 9]. The x-ray interferometer was cut from a crystal slice located between two spheres specifically manufactured to determine the crystal density; in figure 2, this slice ranges from 85 cm to 89 cm. In order to exploit the large displacement capability, the interferometer was designed and manufactured with an unusually long analyzer crystal, the internal designation of which is WS1A (figure 3).

The surface damage produced by grinding was removed by a well-known cupric-ion polishing process of Si wafers [10]. In our variant, the reagents (cupric nitrate and ammonium fluoride) are in water solution. When the interferometer is dipped in that solution, Si undergoes a number of reactions to form soluble silicates and its surface becomes copper plated. Plating, which stops etching, is removed by a solution of iron chloride. Etching is carried out by continuously dipping the interferometer alternately in the two solutions. The advantages of cupric ion etching are that the amount of stock removal is precisely given by the number of etching cycles and that this etching affords a superior geometrical control than the usual HNO_3–HF etching. However, because of anisotropy, the crystal surfaces, though flat on average,

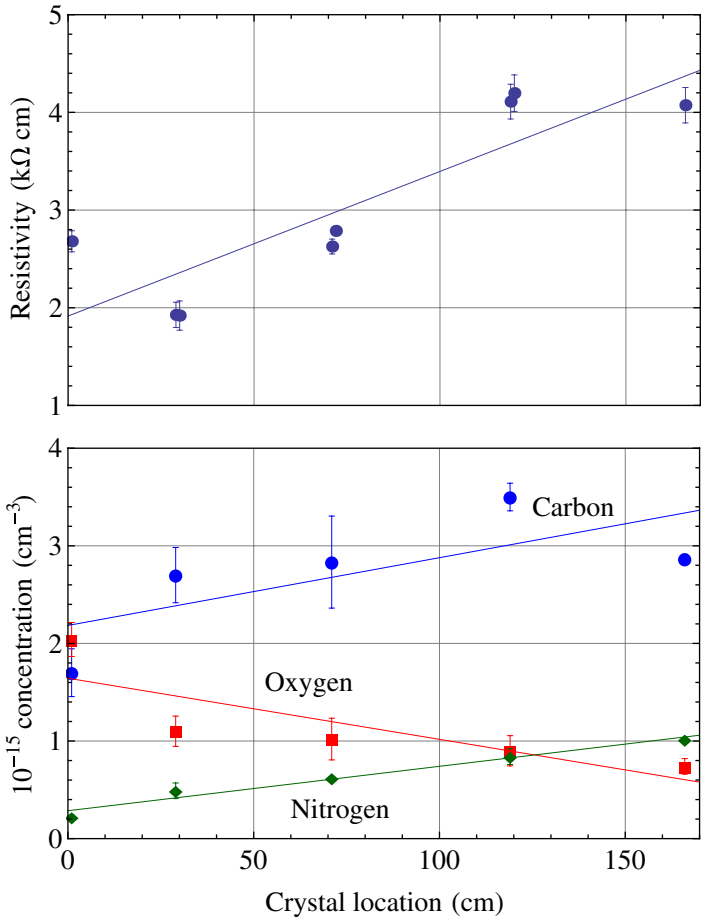

Figure 2. Resistivity (top) and contamination (bottom) of the WASO04 crystal.

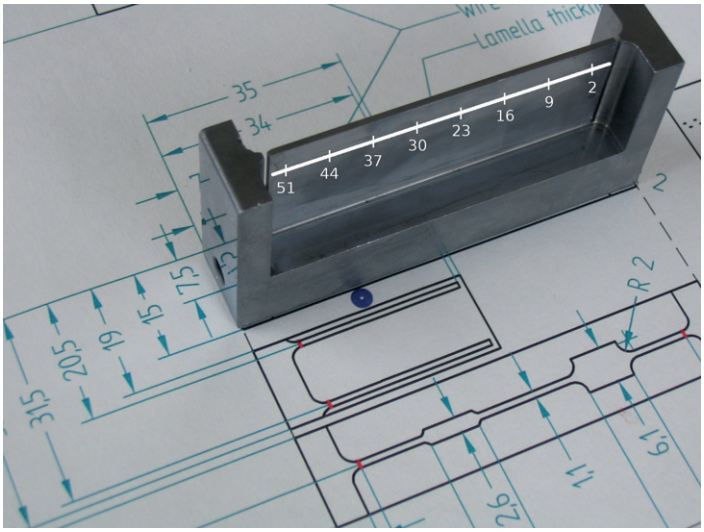

Figure 3. Photograph of the WS1A crystal. The blade size is $(55 \times 20 \times 0.98)$ mm^3.

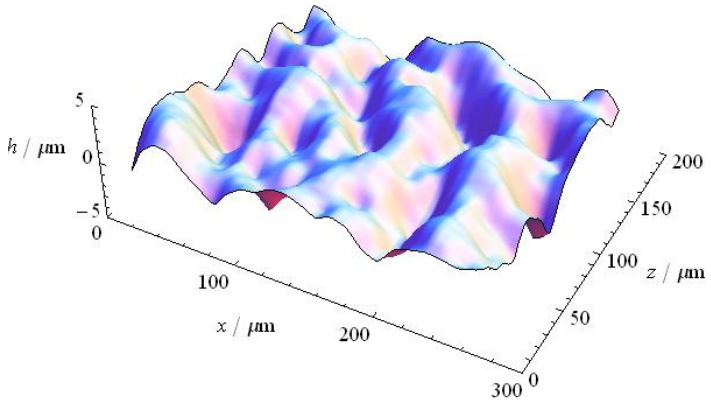

Figure 4. Topography of the analyzer surfaces. The image was obtained by confocal microscopy.

are quite rough. As shown by the topography in figure 4, they display a significant texture with 100 μm length scale and 10 μm peak-to-valley amplitude. The potential influence of surface roughness on the lattice parameter measurement will be discussed in the next section.

3. Lattice spacing measurement

3.1. Measurement procedure

The lattice spacing was determined by comparing the unknown period of the x-ray fringes against the known period of the optical fringes. This is done by measuring the x-ray fringe phases at the ends of increasing analyzer displacements [11, 12]. To measure the x-ray fringe fraction, the least-squares method is applied; the input data are about 300 samples of six fringes, with a 100 ms integration time and a sample duration of 30 s. Since it is not possible to keep the drift between the x-ray and the optical interferometers as small as desirable, the analyzer is repeatedly moved back and forth along any given displacement. Each measurement is typically the average of 9 values collected in measurement cycles lasting 15 min during which the analyzer is moved back and forth by about 1 mm (3000 optical orders or 4.94×10^6 lattice planes).

3.2. Measurement results

Figure 5 (top panel) shows the d_{220} values along the line indicated in figure 3; the measurements were carried out in May and November 2008. It illustrates the first successful operation of a separate-crystal x-ray interferometer over a 5 cm scan. During measurements, the analyzer was shifted step-by-step while the splitter/mirror crystal and the x-rays were maintained fixed. The measurements were carried out over 52 contiguous crystal slices, about 1 mm wide. In order to cope with Abbe's error, in addition to nullifying electronically the crystal rotations [13], the offset between the x-ray and the optical baselines was made harmless by interpolating a vertical sequence of eight d_{220} values to obtain the value having a zero offset [14]. Therefore, the values in figure 5 are averages over vertical strips 14 mm high.

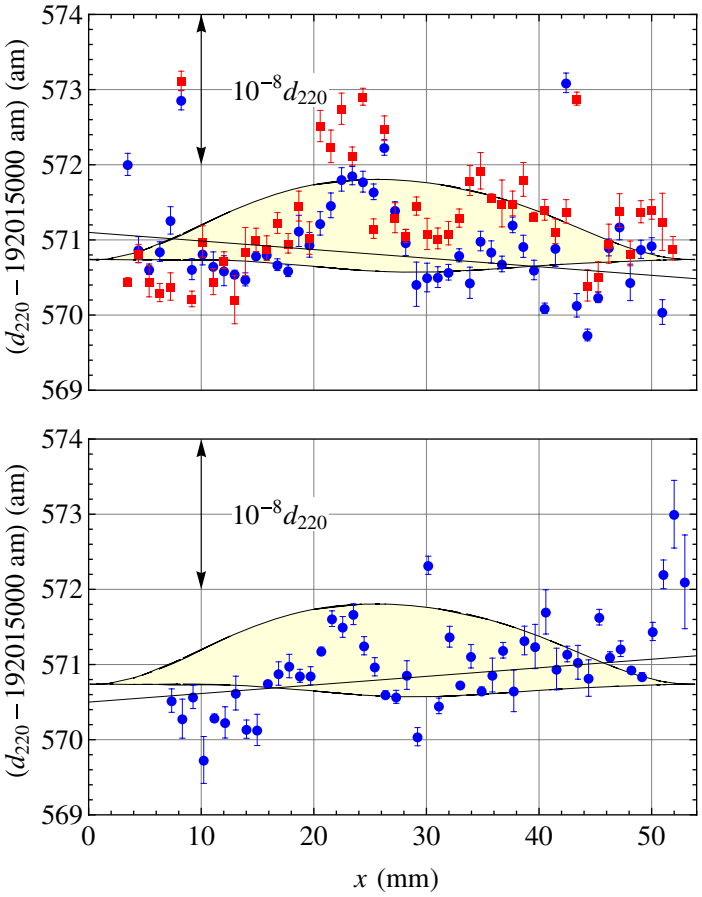

Figure 5. Lattice spacing variation in the WS1A crystal, obverse (top panel) and reverse (bottom panel). Measurements were carried out in May 2008 (blue dots) and November 2008 (red squares). The filled areas enclose the variations due to the self-weight deformation of the analyzer. The lines suggest the trends of the May 2008 data.

The analyzer was designed on the basis of a finite element analysis of elastic bending, as well as of the response to surface stress and thermal loads. In figure 5, the filled areas enclose the expected d_{220} variations due to self-weight deformation. The lower and upper bounds correspond to the analyzer resting on the inner or outer edges of its $(5 \times 5)\,\text{mm}^2$ feet. The minimum strain occurs in the crystal top, but, as the figure shows, it is of the same magnitude as the measurement uncertainty. Our d_{220} measurements should be sensitive enough to detect the self-weight deformation, but other effects are prevailing. Nevertheless, the final measurement result has been corrected for the residual strain.

Figure 5 shows a small drift of the measured values, which makes the data belonging to different surveys fluctuate about different lines. These trends might be due to variations of the laser-beam incidence on the analyzer front mirror. In fact, the interferometer basement rests on three O-rings to insulate it from vibrations, e.g. resonances of the vacuum chamber, but the laser-beam pointer is not on the same base. When the analyzer is displaced—owing to the relatively large mass of the carriage, more than 1 kg—the whole interferometer tilts by about

5 μrad cm^{-1}. Since the incidence angle of the laser beam changes by the same quantity, with an initial misalignment of about $\pm 60\,\mu$rad, the expected variation of the measured value is $\pm 0.3 \times 10^{-9} d_{220}$ cm $^{-1}$, not far from the values observed in figure 5.

Figure 5 shows outliers that require an explanation. It is necessary to separate bulk variations of d_{220}, that is, crystal strains, from apparent variations due to surface imperfections. The x-fringe phase, which is the basic measured quantity, images the crystal surface, as well as any extraneous material on it. Though this phase-contrast image is weaker by orders of magnitude than the lattice image, at the sensitivity level we are operating it could affect the measurement result. To separate false signals from reality, the analyzer crystal was symmetrically designed in order to make it possible to reverse it and to operate it with the entrance and exit surfaces exchanged. Figure 5 (bottom panel) shows the d_{220} values obtained with the analyzer reversed; additional outliers are evident, in different crystal locations.

The short range perfection of the WASO04 crystal was investigated by PTB [5] and INRIM [15] by x-ray topography; the results indicated a perfect crystal structure from the micrometer to the centimeter ranges. Additionally, outliers were not observed in surveys, though not so wide and sensitive, carried out in crystals having a different surface finish [14, 16]. Therefore, though we do not yet have additional experimental evidence, we infer that the outliers do not indicate bulk variations of the lattice spacing. Since the d_{220} measurement is a derivative of the x-fringe phase, a difficulty with this inference is that an outlier indicates a step variation of the relevant influence quantity. In our case, all outliers indicate a d_{220} value greater than expected, that is, a positive derivative. This corresponds to always positive steps, that is, to increase (or decrease) the relevant influence quantity. Though not impossible, this seems unusual.

Figure 5 shows background fluctuations of the lattice parameter that consistently reproduce themselves, but they do not fully repeat when the analyzer is reversed. Additional details are given in figure 6, which shows a contour plot of the lattice strain derived from the observed variations of the x-ray fringe period, assuming that the variation arises from the lattice strain. To obtain the contour plots, the traveling x-ray fringes were recorded by means of a multianode photomultiplier having a vertical pile of eight NaI(Tl) scintillator crystals. Hence, the fringes were processed [15] to obtain a d_{220} value in each of the 8×52 pixels—measuring (1×1.75) mm^2—of figure 5. Basically, the x-ray and optical interference patterns were compared and the lattice strain was inferred from their differences. This inference requires that the optical interference is aberration-free. Therefore, in the figure, all the contributions not ascribable for certain to the x-ray interference have been removed. The figure shows vertical structures that might be a memory of the crystal-grinding pattern; investigations are under way to confirm this hypothesis. The difference between the obverse and reverse images confirms the presence of surface effects. Figure 6 also shows that the outliers of figure 5 correspond to localized structures, with an oscillating shape as expected for the derivative of a phase pulse. This helps to dissolve the difficulties and to explain them.

Figure 7 shows a histogram of the differences between the measured values of the lattice spacing in two different surveys of the lattice strain; the surveyed area is the same as in figure 6 (top panel) and the total pixel number is 416. The extremely good measurement repeatability is to be noted.

To explain why our suspicion lies in surface imperfections, let us consider the simplest case of an imperfect geometry of the analyzer surfaces causing crystal thickness $t_A(x)$, interferometer focusing $z_A(x)$ and effective Bragg's alignment $\theta_A(x)$ to depend on the displacement x. In this

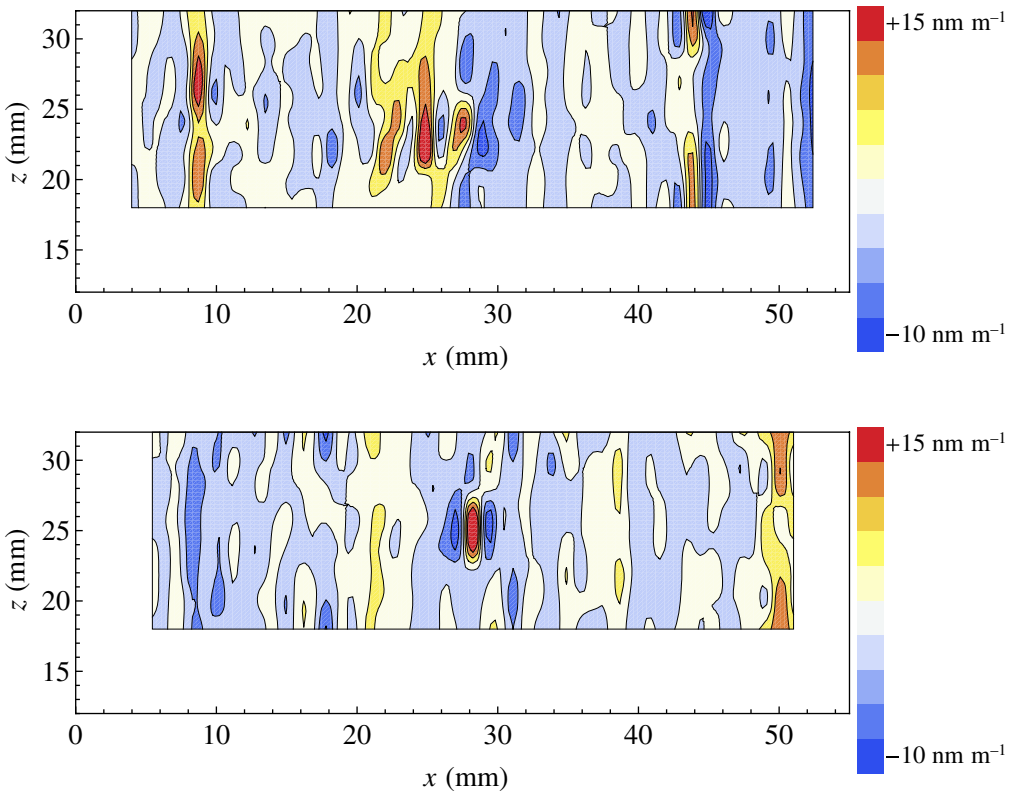

Figure 6. Contour plot of the observed relative variations (real or apparent) of the lattice parameter in the WS1A crystal, obverse (top panel) and reverse (bottom panel). The frames indicate the actual crystal shape and size.

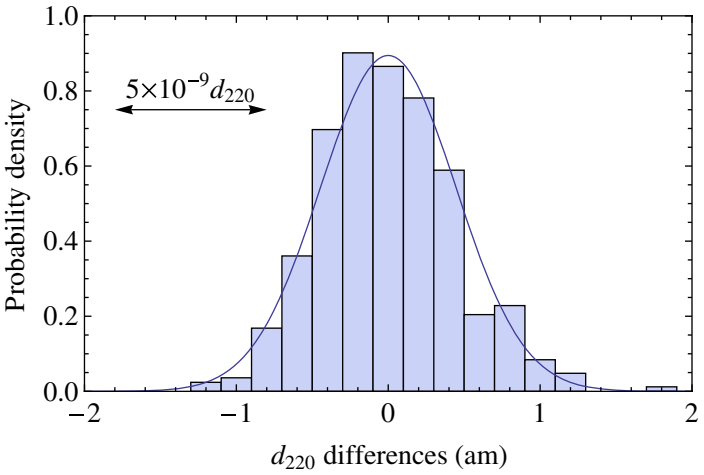

Figure 7. Histogram of the differences between the d_{220} values measured in the 2008-11-10 and 2008-11-12 surveys, in the 416 pixels of figure 6. The standard deviation of the data is 0.45 am (corresponding to $2.3 \times 10^{-9} d_{220}$). The solid line is the best fit normal distribution.

Table 2. The WASO04 crystal—corrections and uncertainties of d_{220}.

Contribution	Correction 10^{-9}	Uncertainty 10^{-9}
Statistic	0.0	0.5
Wavelength	−3.0	1.5
Laser beam diffraction	7.3	0.7
Laser beam alignment	1.3	1.3
Abbe's error	0.0	2.5
Trajectory	−6.0	0.3
Temperature	−0.5	3.0
Self-weight	−3.1	1.8
Aberrations	0.0	2.0
Total	−4.0	5.2

case, the phase of the interferometer signal,

$$I \sim \cos\left[hx + at_{\mathrm{A}}(x) + bz_{\mathrm{A}}(x) + c\theta_{\mathrm{A}}(x)\right], \tag{2}$$

is no longer proportional to the number of traveled lattice planes [17, 18]. In equation (2), $h = 2\pi/d_{220}$, $a = -30\,\mathrm{mrad}\,\mu\mathrm{m}^{-1}$, $b = -60\,\mathrm{mrad}\,\mu\mathrm{m}^{-1}$ and $c = 30\,\mathrm{mrad}\,\mu\mathrm{rad}^{-1}$ are sensitivity coefficients. For example, a $4\,\mu$m 'resonance' of thickness and focusing variations brings about an apparent d_{220} variation as large as $3 \times 10^{-9} d_{220}$, over a displacement of 1 mm. In addition, owing to surface roughness, (2) should also include asymmetry effects due to local non-orthogonal crystal cutting. To clarify the influence of surface geometry on interferometer operation, a theoretical investigation is under way.

A detailed discussion of corrections and of uncertainty contributions listed in table 2 can be found in [14, 16]. In addition, we checked that the laser beam—65% of the optical power, about 0.3 mW, is absorbed by the analyzer—does not cause any significant thermal gradient between the part where d_{220} is measured and the base where the crystal temperature is measured. This test was performed by measurement repetitions with different laser powers: without any readjustment of the experimental apparatus, in the same crystal location and on the same working day. The results shown in figure 8 indicate that any gradient is below our present measurement sensitivity. The figure also shows the excellent short-term repeatability of the measurements.

4. Conclusions

After the corrections and the uncertainty contributions listed in table 2 were taken into account the values shown in figure 5 were averaged. The final lattice-spacing value in vacuum and at 22.5 °C is

$$d_{220}(\mathrm{WASO04}) = 192.015\,570\,2(10)\,\mathrm{pm}. \tag{3}$$

The value in equation (3) is not corrected for carbon and oxygen contamination. Consequently, the carbon and oxygen contributions to the error budget were not taken into account.

A summary of the available measurement values is shown in figure 9. It compares the values obtained by extrapolation from the residual carbon and oxygen contamination and from x-ray double crystal diffractometry. The WS5C 2006 value is given in [7]. It was measured

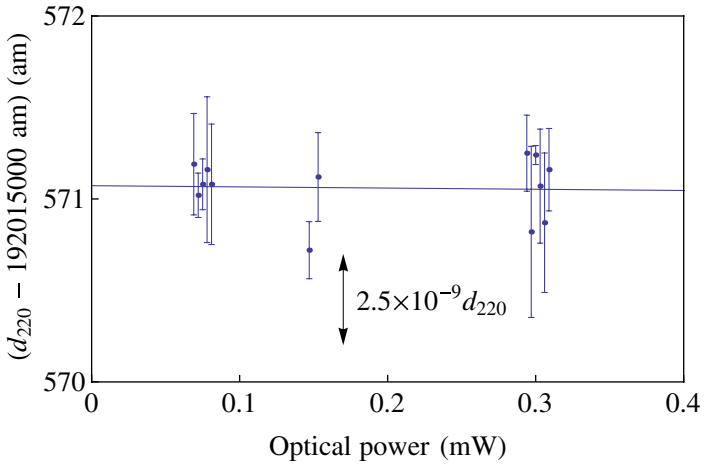

Figure 8. Measured value of d_{220} with different laser-beam powers; no thermal-load effect is visible.

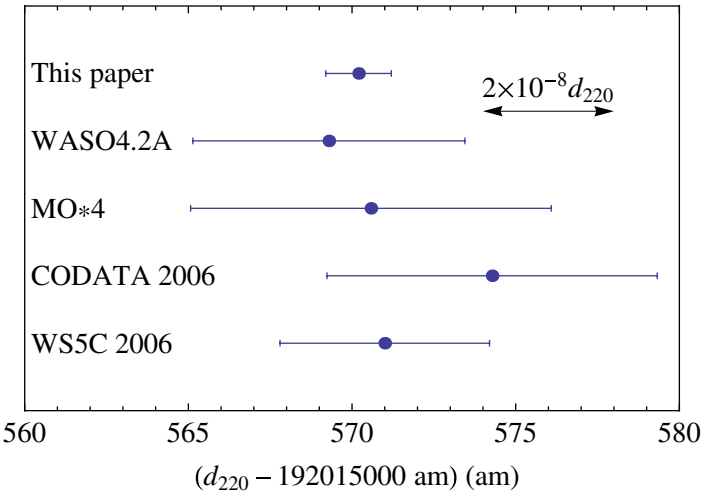

Figure 9. Measurement values of the mean (220) lattice plane spacing in the WASO04 crystal.

by means of a different experimental apparatus and a different x-ray interferometer, named WS5C, still manufactured from the same WASO04 ingot. The CODATA value is obtained correcting the lattice spacing value recommended by the Committee on Data for Science and Technology [4] for a non-contaminated crystal, for the carbon, oxygen and nitrogen content of WASO04 (see table 1) [5]. The remaining two values are obtained by combining the more recent determinations of the lattice parameter of the WASO 4.2A and the MO*4 crystals [14, 16] with the fractional differences observed by PTB when comparing the lattice spacings of WASO04 and WASO4.2A (respectively MO*4) [19]. All measured and calculated values agree within their standard uncertainty.

Although, for the mentioned reasons, we had to exclude some data, a comparison with the results in [14, 16] evidences the enhanced performances of the experimental apparatus and, in particular, the better crystal and interferometer quality. Anomalies and outliers are now clearly evident because of the extended measurement range and noise reduction, below $10^{-8}d_{220}$. Our

observations suggest technological and theoretical investigations in the field of the operation, design and manufacturing of the x-ray interferometer and, more generally, of transmission optics for x-rays.

Acknowledgments

This work received funds from the European Community's Seventh Framework Programme ERA-NET Plus—(grant 217257), the Regione Piemonte—(grant D64) and the Compagnia di San Paolo.

References

[1] Becker P, De Bièvre P, Fujii K, Glaeser M, Inglis B, Luebbig H and Mana G 2007 Considerations on future redefinitions of the kilogram, the mole and of other units *Metrologia* **44** 1–14
[2] Becker 2003 Tracing the definition of the kilogram to the Avogadro constant using a silicon single crystal *Metrologia* **40** 366–75
[3] Becker P *et al* 2006 Large production of highly enriched Si-28 for the precise determination of the Avogadro constant *Meas. Sci. Technol.* **17** 1854–60
[4] Mohr P J, Taylor B N and Newell D B 2008 CODATA recommended values of the fundamental physical constants: 2006 *Rev. Mod. Phys.* **80** 633–730
[5] Becker P, Bettin H, Danzebrink H-U, Glaeser M, Kuetgens U, Nicolaus A, Schiel D, De Bièvre P, Valkiers S and Taylor P 2003 Determination of the Avogadro constant via the silicon route *Metrologia* **40** 271–87.
[6] Fujii K *et al* 2005 Present state of the Avogadro constant determination from silicon crystals with natural isotopic compositions *IEEE Trans. Instrum. Meas.* **54** 854–9
[7] Becker P, Cavagnero G, Kuetgens U, Mana G and Massa E 2007 Confirmation of INRiM and PTB determinations of the Si lattice parameter *IEEE Trans. Instrum. Meas.* **56** 230–4
[8] Becker P 1999 The determination of the Avogadro constant—not simply a metrological problem *IEEE Trans. Instrum. Meas.* **48** 2259
[9] Kessler E G, Owens S M, Henins A and Deslattes R D 1999 Silicon lattice comparisons related to the Avogadro project: uniformity of new material and surface preparation effects *IEEE Trans. Instrum. Meas.* **48** 221–4
[10] Mendel E and Yang K-H 1969 Polishing of silicon by the cupric ion process *Proc. IEEE* **57** 1476–80
[11] Becker P and Mana G 1994 The lattice parameter of silicon: a survey *Metrologia* **31** 203–9
[12] Basile G, Bergamin A, Cavagnero G, Mana G, Vittone E and Zosi G 1995 Comparison of INRIM and PTB lattice-spacing standards *IEEE Trans. Instrum. Meas.* **44** 526–9
[13] Bergamin A, Cavagnero G and Mana G 1993 A displacement and angle interferometer with subatomic resolution *Rev. Sci. Instrum.* **64** 3076–81
[14] Ferroglio L, Mana G and Massa E 2008 Si lattice parameter measurement by centimeter x-ray interferometry *Opt. Express* **16** 16877–88
[15] Bergamin A, Cavagnero G, Mana G, Massa E and Zosi G 2000 Measuring small lattice distortions in Si-crystals by phase-contrast x-ray topography *J. Phys. D: Appl. Phys.* **33** 2678–82
[16] Massa E, Mana G and Kuetgens U 2009 Comparison of the INRIM and PTB lattice-spacing standards *Metrologia* **46** 249–253
[17] Mana G and Vittone E 1997 Scanning LLL x-ray interferometry. II. Aberration analysis *Z. Phys.* B **102** 197–206
[18] Basile G, Bergamin A, Cavagnero G, Mana G, Vittone E and Zosi G 1991 Silicon lattice constant: limits in IMGC X-ray/optical interferometry *IEEE Trans. Instrum. Meas.* **40** 98–102
[19] Martin J, Kuetgens U, Stuempel J and Becker P 1998 The silicon lattice parameter—an invariant quantity of nature? *Metrologia* **36** 811–7